

# Aqueous-Phase Photooxidation of Vanillic Acid: A Potential Source of Humic-Like Substances (HULIS)

Shanshan Tang, Fenghua Li, Narcisse T. Tsona, Chunying Lu, Xinfeng Wang, and Lin Du\*

Cite This: *ACS Earth Space Chem.* 2020, 4, 862–872

Read Online

ACCESS |



Metrics &amp; More



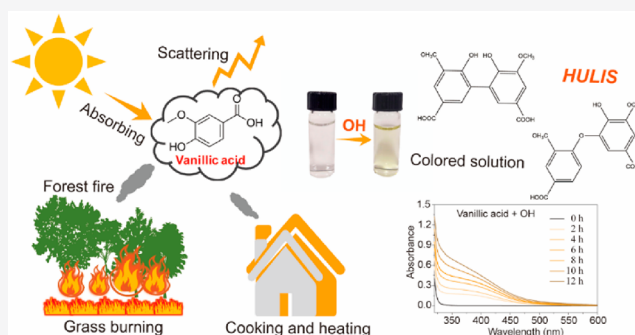
Article Recommendations



Supporting Information

**ABSTRACT:** Phenolic compounds are emitted in large amounts from biomass burning and can undergo aqueous-phase reactions in the atmosphere to form secondary organic aerosols (aqSOA). In this study, the kinetics and products of the reaction of vanillic acid (VA) with hydroxyl radicals (OH) were characterized, and their formation mechanisms were determined using ultrahigh-performance liquid chromatography ultraviolet/mass spectrometry (HPLC-UV/MS) and UV–vis absorption and fluorescence spectroscopies. The obtained rate constants of the VA + OH reaction are  $(9.8 \pm 1.5) \times 10^9$  and  $(3.8 \pm 0.7) \times 10^9 \text{ M}^{-1} \text{ s}^{-1}$  at pH 2 and 10, respectively. A yellowish solution is obtained after illumination, and it absorbs in the UV–vis region and has an unusual fluorescence spectrum, which suggests formation of a humic-like substance (HULIS) by the C–C and C–O coupling of phenoxyl radicals. Additionally, hydroxylation of the aromatic ring occurs through OH addition, which increases the degree of oxidation of the products. This study indicates that the aqueous-phase OH oxidation of phenolic acid compounds may contribute to formation of HULIS in the atmosphere, especially in areas with active burning of biomass. The high-molecular-weight products would remain in the particle phase after fog/cloud evaporation and influence the chemical and optical properties of atmospheric particles.

**KEYWORDS:** biomass burning emissions, aqueous-phase photooxidation, kinetics, HULIS, reaction mechanism, optical property



## INTRODUCTION

Secondary organic aerosols (SOA) are predominantly formed by oxidation of volatile organic compounds (VOCs), which results in a reduction in the saturation vapor pressure, and the subsequent nucleation or partitioning of the oxidation products onto preexisting particles.<sup>1,2</sup> Although most studies have focused on gas-phase photochemical processes, aqueous-phase reactions are also important contributors to SOA (aqSOA) in clouds, fogs, or wet aerosol particles. The aqueous-phase processes are driven by a combination of biogenic and anthropogenic emissions and can significantly affect aerosol composition and properties.<sup>3–6</sup> These poorly characterized aqueous-phase processes can at least partially account for the large discrepancies between air quality models and field observations.<sup>2,4,7</sup> It is necessary to establish an accurate aqueous-phase model for effective air quality management.<sup>6</sup> Therefore, understanding the formation and transformation of aqSOA is important for determining the atmospheric evolution of particles and estimating their impacts on climate.

Biomass burning releases substantial amounts of organic compounds into the atmosphere and is a significant source of primary organic aerosols and SOA precursors.<sup>8</sup> Levoglucosan and methoxyphenolic compounds have been used as

biomarker tracers of organic aerosols from biomass burning due to their unique signatures.<sup>9,10</sup> In addition, phenols and methoxyphenols contribute to approximately 20–40% of the particulate mass from hardwood and softwood burning.<sup>11</sup> Biomass burning mixtures are rapidly oxidized by hydroxyl radicals (OH) in the aqueous phase, leading to formation of aqSOA with high mass yields.<sup>12–14</sup> The aqSOA formed by residential wood combustion can account for 4–20% of the total organic aerosol emissions in Europe.<sup>7</sup> The average O/C ratios of aqSOA from phenols is approximately 1, which means that they are highly oxidized.<sup>15</sup> In addition, these aqSOA include numerous water-soluble molecules with polar functional groups (–C=O, –COOH, and –OH),<sup>16,17</sup> which indicates that phenolic aqSOA have the potential to affect the particle hygroscopicity and cloud formation.

Humic-like substances (HULIS) have been detected in peat, tar ball, biomass materials, and fossil fuels,<sup>18–20</sup> constituting a

Received: March 12, 2020

Revised: April 25, 2020

Accepted: May 4, 2020

Published: May 5, 2020



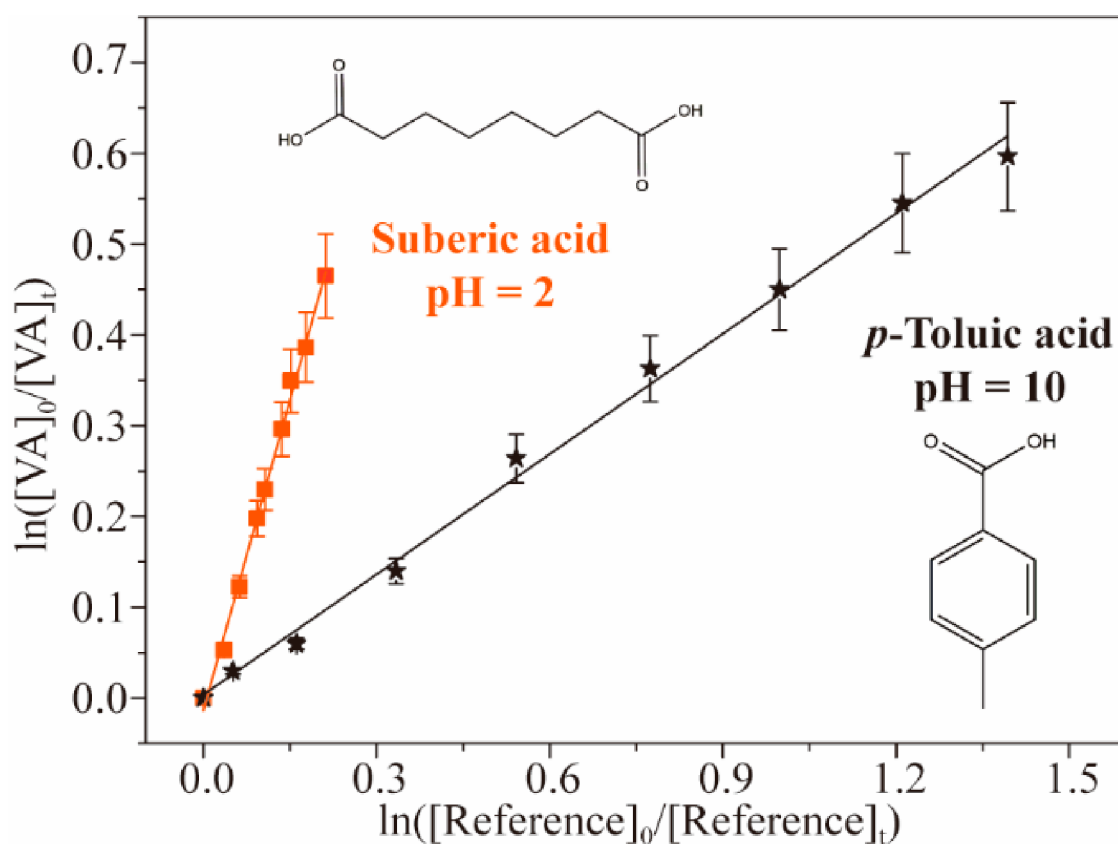


**Figure 1.** Relative kinetic data for vanillic acid oxidized by OH radicals in the aqueous phase under acidic and basic conditions.

significant fraction of water-soluble organic carbon and contributing to the light-absorbing properties of organic aerosols. Moreover, the aqueous OH-initiated oxidation of phenolic compounds has been shown to form products that have brown carbon (BrC) characteristics.<sup>7,21,22</sup> 3,5-Dihydroxybenzoic acid, a water-soluble compound emitted by biomass burning, has been demonstrated to react with OH radicals to form light-absorbing organic matter.<sup>23</sup> Gelencsér and co-workers attributed the light absorption to formation of HULIS and proposed that HULIS may have a secondary origin from aqueous oxidation products, in addition to the primary origin.<sup>23</sup> Irradiation of hydrogen peroxide ( $H_2O_2$ ) and phenolic compounds led to formation of a colored solution, which is similar to HULIS found in atmospheric particulate matter.<sup>24</sup> This reaction proceeded more rapidly for an *o*-methoxy-substituted compound, suggesting that the radical coupling of phenols and methoxyphenolic compounds may contribute to HULIS in tropospheric waters.<sup>24</sup> Furthermore, the chemical composition and yield of aqSOA formed by the photolysis and OH oxidation of vanillin were investigated.<sup>12</sup> Although the optical properties of aqSOA were not quantified, a yellowish solution was obtained. The dimeric products of vanillin oxidation can absorb light.<sup>12</sup> Recently, the photo-induced oligomerization of phenolic compounds (vanillin and acetosyringone) yielded products with humic-like fluorescence properties that were assumed to be HULIS.<sup>25</sup> However, irradiation of vanillic acid (VA), *m*-cresol, and guaiacol did not yield HULIS or oligomers,<sup>25</sup> demonstrating that they could hardly undergo photolysis.

To date, oxidation of phenolic acids, which are also an important fraction of biomass burning products, has been

rarely studied. For example, vanillic, syringic, and *p*-hydroxybenzoic acids have been used as tracers of biomass burning emissions.<sup>10,26</sup> VA was also identified in single tar ball particles by laser desorption/resonance-enhanced multiphoton ionization mass spectrometry.<sup>20</sup> In the atmosphere above forests, the concentration of vanillic acid could reach up to  $6500 \text{ ng m}^{-3}$ .<sup>10</sup> The detected atmospheric concentration of VA was approximately  $2\text{--}3 \text{ ng m}^{-3}$  in Beijing during the APEC summit.<sup>27</sup> More recently, ice core records of vanillic acid from Aurora Peak in Alaska since the 1660s show that the largest concentration was approximately 0.035 ppb.<sup>28</sup> In this work, a photoreactor was used to simulate the photooxidation of VA in cloud or fog droplets and evaluate its potential contributions to formation of HULIS.

## EXPERIMENTAL SECTION

**Chemicals.** Vanillic acid (>98.0%), suberic acid (>99.0%), and *p*-toluic acid (>98.0%) were purchased from Tokyo Chemical Industry (TCI) and used as received without further purification. Acetonitrile and formic acid (Optima LC/MS grade), which were used for the liquid chromatography mobile phase, were obtained from Fisher Scientific. All solutions were freshly prepared with purified water from a Millipore Milli-Q purification system ( $18.2 \text{ M}\Omega \text{ cm}^{-1}$  resistivity at  $25 \text{ }^\circ\text{C}$ ). In addition, hydrochloric acid and sodium hydroxide solutions were used to adjust the pH. All solutions were freshly prepared for each experimental run.

**Kinetic Experiments.** In the field of aqueous-phase kinetics, the relative rate technique is widely used to determine the rate constant for two reasons: it does not involve the OH radical concentration, and the reactant concentration does not

need to be accurately known.<sup>29</sup> Therefore, the relative rate technique was used to investigate the rate constant of the reaction of VA with OH radicals in this study. Though for kinetic and product experiments, the same<sup>30,31</sup> or different light sources<sup>32,33</sup> were used, in this study we used the same lamp in all experiments. This method relies on the assumption that VA and the reference compounds are removed solely by reacting with OH radicals. VA was mixed with the reference compound in the same reactor, and the rate constant was obtained by detecting the relative losses of VA and the reference compounds, which have well-known OH rate constants. The rate constant was calculated by

$$\ln\left(\frac{[\text{VA}]_0}{[\text{VA}]_t}\right) = \frac{k}{k_{\text{ref}}}\ln\left(\frac{[\text{ref}]_0}{[\text{ref}]_t}\right) \quad (1)$$

where  $[\text{VA}]_0$  and  $[\text{VA}]_t$  are the concentrations of VA before illumination (time = 0) and during illumination (time =  $t$ ). The variables  $[\text{ref}]_0$  and  $[\text{ref}]_t$  are the concentrations of the reference compounds at time = 0 and time =  $t$ . A straight line with a slope of  $k/k_{\text{ref}}$  was obtained by plotting  $\ln([\text{VA}]_0/[\text{VA}]_t)$  versus  $\ln([\text{ref}]_0/[\text{ref}]_t)$  (Figure 1).

The typical pH values of polluted cloud, polluted fog, and marine aerosols are 2–5, 2–7, and 1–9, respectively.<sup>4</sup> As a carboxylic acid, VA exists in different forms, i.e., the protonated acid and corresponding deprotonated ion forms, under acidic and basic conditions, respectively, and this phenomenon is controlled by its  $\text{p}K_{\text{a}}$  value. At  $\text{pH} < 4$ , VA is found in its protonated form, and it exists in its deprotonated form at  $\text{pH} > 9$ .<sup>34,35</sup> Taking these facts into consideration, pH 2 and 10 were chosen for the acidic and basic conditions for these experiments. Suberic acid (SA,  $k = (4.8 \pm 0.4) \times 10^9 \text{ M}^{-1} \text{ s}^{-1}$ ) and *p*-toluic acid (TA,  $k = (8.0 \pm 0.8) \times 10^9 \text{ M}^{-1} \text{ s}^{-1}$ )<sup>36</sup> were chosen as the acidic and basic reference compounds, respectively, to study the kinetics of the VA + OH reaction.

Aqueous photochemical experiments were conducted in a 250 mL quartz glass vessel with a path length of 7 cm, and 200 mL of solution was initially used for the reaction. Each experiment was completed within 2 h. The solution was continuously stirred with a magnetic stir bar and irradiated with two 254 nm UV lamps to generate OH radicals by hydrogen peroxide ( $\text{H}_2\text{O}_2$ ) photolysis. The emission spectrum of the used UV lamp was provided in the Supporting Information (Figure S1). As previously reported, the steady-state concentration of OH radicals can be estimated by dividing the average rate constant of VA loss ( $k'$ ) by the bimolecular rate constant of VA oxidation by OH ( $k_{\text{VA+OH}} = 9.8 \times 10^9 \text{ M}^{-1} \text{ s}^{-1}$ )<sup>17</sup>

$$[\text{OH}] = \frac{k'}{k_{\text{VA+OH}}} \quad (2)$$

Considering the different rate constants at pH 2 and 10, the steady-state OH radical concentration was estimated to be approximately  $10^{-14} \text{ M}$ . To accurately determine the rate constants for the reaction of VA with OH radicals at pH 2 and 10, kinetics experiments were performed three times at each pH by adjusting the concentration ratio of VA and the reference compounds. The initial VA concentrations were 0.5 and 1 mM. For product identification, the experiments were conducted at VA concentrations of 0.5 and 5 mM, and the corresponding concentrations of  $\text{H}_2\text{O}_2$  were 10 and 100 mM, respectively. The  $\text{H}_2\text{O}_2$  solution was added to the VA solution and well mixed before turning on the UV light to initiate the

radical reaction. To verify that the VA + OH reaction follows first-order kinetics during the measurement, the loss of VA in the aqueous phase was measured as the reaction progressed (Figure S2 in the Supporting Information). During the experiments, approximately 60% and 90% of VA were consumed in the aqueous phase at pH 2 and 10, respectively. The kinetic experiments and product detection in this study were completed within 2 h.

**HPLC-UV/MS Analysis.** During the kinetic experiments, 1 mL of the sample solution was removed from the 200 mL reaction mixture at given times, and the concentrations of VA and the reference compounds were measured by HPLC (UltiMate 3000, Thermo Scientific, USA). In one experiment, a total of 8 mL of solution was removed from the 200 mL of solution, and the removed solution had a negligible effect on the kinetic experiment. The HPLC system consisted of a UV-vis detector and an ISQ EC mass spectrometer (MS, Thermo Scientific, USA) equipped with an electrospray ionization (ESI) source. Separation was performed using a Thermo Scientific C18 column (150 mm  $\times$  2.1 mm, 3  $\mu\text{m}$ , 100  $\text{\AA}$ ) kept at 30  $^\circ\text{C}$ . A formic acid solution in water (pH 2.8) (mobile phase A) and acetonitrile (ACN) (mobile phase B) was delivered at a flow rate of 0.2 mL  $\text{min}^{-1}$ , and the injection volume was set to 5  $\mu\text{L}$ . Mass spectra were obtained in both the total ion current (TIC, 50–700  $m/z$ ) and the selected ion monitoring (SIM) modes. The ESI conditions included a capillary voltage of  $-2.0 \text{ kV}$  and source temperature of 300  $^\circ\text{C}$ , and nitrogen was used as the sheath gas ( $2 \times 10^5 \text{ Pa}$ ), auxiliary gas ( $2 \times 10^4 \text{ Pa}$ ), and collision gas. The gradient elution programs for kinetic analysis and product identification are shown in Table S1 in the Supporting Information. The total retention times were 25 and 55 min. The concentration of VA was quantified using the calibration curve based on the HPLC-UV signals at 290 nm.

**Ultraviolet-Visible (UV-vis) Spectroscopy.** UV-vis absorption spectra of the samples were collected using a double-beam UV-vis spectrophotometer (P9, Shanghai Mapada, China) in the range of 200–800 nm. The background spectrum was measured using purified water to obtain the baseline. After illumination, 3 mL of the sample was removed from the vessel at regular intervals. The sample was then pipetted into a quartz cuvette with an optical length of 10 mm to measure the absorption of the colored products for the UV-vis spectral analysis. The concentration of VA used in the UV-vis spectral study was 0.2 mM (Figure S3). Moreover, an additional experiment was performed with 5 mM VA + OH radicals to observe the reaction process in the visible region.

**Fluorescence Excitation-Emission Matrix (EEM) Analysis.** The 3 mL of sample used in the UV-vis spectral analysis was transferred to a 10 mm quartz cuvette for fluorescence measurements using a spectrofluorophotometer (F-320, Tianjin Gangdong, China). The fluorescence excitation-emission matrix (EEM) was obtained under the following conditions: excitation and emission wavelength ranges were set to 200–600 and 220–700 nm; scanning intervals were set to 5 and 2 nm, respectively; slit widths were all fixed at 10 nm; and scan speeds were set to 30 000 nm  $\text{min}^{-1}$ . The fluorescence features in this study were identified based on the main characteristics in the literature.<sup>19,24,25,37–39</sup>

**Error Analysis and Control Experiments.** For comparison, the following two control experiments at pH 2 were performed to demonstrate that the loss of vanillic acid was only due to photooxidation by OH radicals: (1) a dark control

**Table 1.** Rate Constants for Reactions of Carboxylic Acid Compounds and Aromatic Compounds with OH Radicals in the Aqueous Phase

	reactant	pH	rate constants ( $M^{-1} s^{-1}$ )	ref
carboxylic acids	<i>cis</i> -pinonic acid	2	$(3.6 \pm 0.3) \times 10^9$	Witkowski and Gierczak <sup>41</sup>
		10	$(3.0 \pm 0.3) \times 10^9$	
	limonic acid	2	$(1.3 \pm 0.3) \times 10^{10}$	Witkowski et al. <sup>31</sup>
		10	$(5.7 \pm 0.6) \times 10^9$	
	$\beta$ -caryophyllonic acid	2	$(4.2 \pm 0.5) \times 10^{10}$	Witkowski et al. <sup>30</sup>
		8	$(6.5 \pm 0.7) \times 10^9$	
vanillic acid	2	$(9.8 \pm 1.5) \times 10^9$	this work	
	10	$(3.8 \pm 0.7) \times 10^9$		
aromatics	dimethyl phthalate	6	$3.4 \times 10^9$	Wu et al. <sup>68</sup>
		10	$(2.7 \pm 0.3) \times 10^9$	Wen et al. <sup>69</sup>
	diethyl phthalate	10	$(4.0 \pm 0.2) \times 10^9$	Wen et al. <sup>69</sup>
		7	$(5.9 \pm 0.5) \times 10^9$	Ayatollahi et al. <sup>70</sup>
	salicylic acid	7	$(1.1 \pm 0.1) \times 10^{10}$	Ayatollahi et al. <sup>70</sup>
		5.8	$8.1 \times 10^9$	Venu et al. <sup>71</sup>
	thymol	>13.5	$1.1 \times 10^9$	Venu et al. <sup>71</sup>
		phenol	2	$(1.8 \pm 0.3) \times 10^9$
	5		$(1.5 \pm 0.5) \times 10^{10}$	Smith et al. <sup>42</sup>
	6		$(1.3 \pm 0.9) \times 10^{10}$	Buxton et al. <sup>36</sup>
	catechol	2	$(2.5 \pm 0.3) \times 10^9$	Smith et al. <sup>42</sup>
		5	$(6.9 \pm 2.4) \times 10^9$	Smith et al. <sup>42</sup>
		9	$1.1 \times 10^{10}$	Buxton et al. <sup>36</sup>
	resorcinol	2	$(1.6 \pm 0.1) \times 10^9$	Smith et al. <sup>42</sup>
		5	$(5.8 \pm 1.3) \times 10^9$	Smith et al. <sup>42</sup>
		5.6–6.0	$(1.5 \pm 0.2) \times 10^{10}$	He et al. <sup>32</sup>
	hydroquinone	9	$1.2 \times 10^{10}$	Buxton et al. <sup>36</sup>
		2	$(1.4 \pm 0.2) \times 10^{10}$	Smith et al. <sup>42</sup>
		5	$(1.1 \pm 0.8) \times 10^{10}$	Smith et al. <sup>42</sup>
	guaiaacol	9	$2.9 \times 10^{10}$	Buxton et al. <sup>36</sup>
		2	$(6.8 \pm 0.3) \times 10^9$	Smith et al. <sup>42</sup>
		5	$(1.6 \pm 0.5) \times 10^{10}$	Smith et al. <sup>42</sup>
	3-methoxyphenol	6	$2.0 \times 10^{10}$	Buxton et al. <sup>36</sup>
		5.6–6.0	$(1.1 \pm 0.1) \times 10^{10}$	He et al. <sup>32</sup>
		5.6–6.0	$(1.4 \pm 0.1) \times 10^{10}$	He et al. <sup>32</sup>
	syringol	2	$(1.5 \pm 0.3) \times 10^{10}$	Smith et al. <sup>42</sup>
		5	$(2.0 \pm 0.4) \times 10^{10}$	Smith et al. <sup>42</sup>
		6	$2.6 \times 10^{10}$	Buxton et al. <sup>36</sup>
	2-ethylphenol	5.6–6.0	$(1.7 \pm 0.4) \times 10^{10}$	He et al. <sup>32</sup>
		5.6–6.0	$(1.1 \pm 0.1) \times 10^{10}$	He et al. <sup>32</sup>
5.6–6.0		$(1.7 \pm 0.4) \times 10^{10}$	He et al. <sup>32</sup>	
creosol	5.6–6.0	$(1.7 \pm 0.4) \times 10^{10}$	He et al. <sup>32</sup>	
	5.6–6.0	$(1.7 \pm 0.4) \times 10^{10}$	He et al. <sup>32</sup>	
4-(2-methoxyethyl)phenol	5.6–6.0	$(1.7 \pm 0.4) \times 10^{10}$	He et al. <sup>32</sup>	
	5.6–6.0	$(1.9 \pm 0.4) \times 10^{10}$	He et al. <sup>32</sup>	
3-methoxycatechol	5.6–6.0	$(1.9 \pm 0.4) \times 10^{10}$	He et al. <sup>32</sup>	

experiment without illumination to ensure that VA did not react with  $H_2O_2$  and (2) a direct photodegradation control experiment without  $H_2O_2$  to determine whether or not VA would undergo direct photolysis. The results of the control experiments confirm that no decay occurs during the dark experiment, but  $\sim 7\%$  VA is reduced after 2 h irradiation (Figure S4). A previous study of the photoreactivity of typical phenolic compounds also showed no transformation of VA in dark control experiments.<sup>25</sup>

The total errors,  $\sigma_{VA}$  of the  $k$  values obtained by the relative rate method are approximately 15%, taking into account the precision of the linear regression analysis (eq 1) and the error in the  $k$  and  $k_{ref}$  measurements

$$\sigma_{VA} = k_{VA} \sqrt{\left[ \frac{2\sigma_{k_{VA}/k_{ref}}}{k_{VA}/k_{ref}} \right]^2 + \left[ \frac{\sigma_{k_{ref}}}{k_{ref}} \right]^2} \quad (3)$$

Considering the uncertainty of the experiments (chromatographic peak area integration), the quoted errors of  $k_{VA}/k_{ref}$  are twice the standard error ( $2\sigma_{k_{VA}/k_{ref}}$ ) in the linear least-squares fit of the measured losses. The photodegradation of VA is minor and within the uncertainty of the experiment. Additionally, a linear fit is shown in the calibration curves of the VA concentration versus the HPLC–UV signals (Figure S5), but the calibration errors are ignored here because the relative measurement is independent of the absolute concentrations of the reactants.<sup>40</sup>

## RESULTS AND DISCUSSION

**Rate Constant Measurements for the Reaction of Vanillic Acid with OH Radicals.** Two forms of VA, the protonated form ( $-COOH$ ) and the carboxylate anion ( $-COO^-$ ), exist in the aqueous phase. In previous studies, different rate constants were measured for reactions of the

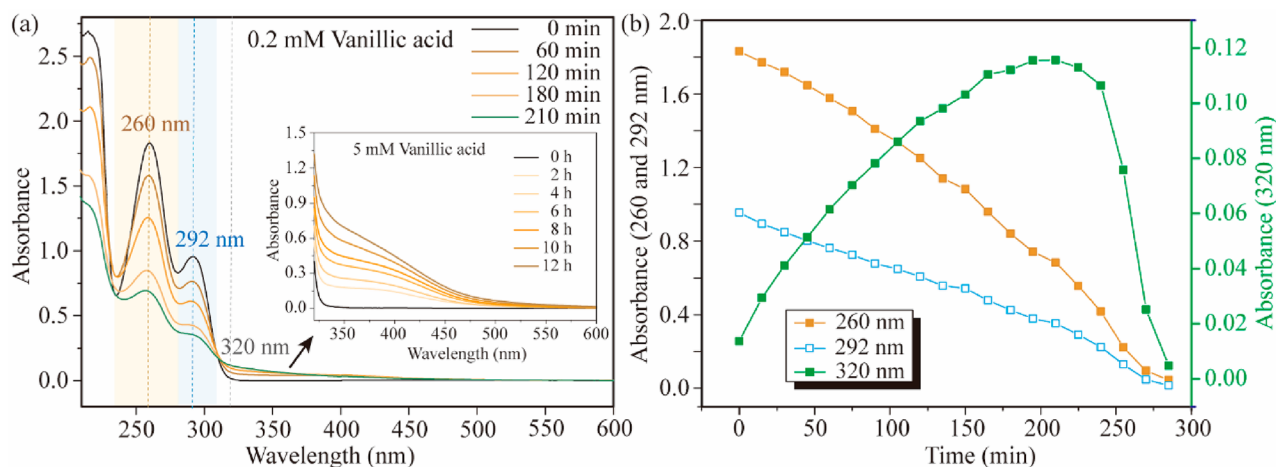


**Figure 2.** (a) UV-vis absorption spectra of 0.2 mM vanillic acid oxidized by OH radicals in the aqueous phase at pH 2 at different reaction times. (Inset) Enlarged spectra at  $\lambda > 320$  nm with a larger vanillic acid concentration (5 mM). (b) Absorption changes of vanillic acid at  $\lambda = 260$ , 292, and 320 nm over different reaction times.

protonated and carboxylate anion forms with OH radicals; for example, the measured rate constants of the *cis*-pinonic acid (CPA) + OH reaction were  $(3.6 \pm 0.3) \times 10^9 \text{ M}^{-1} \text{ s}^{-1}$  at pH 2 and  $(3.0 \pm 0.3) \times 10^9 \text{ M}^{-1} \text{ s}^{-1}$  at pH 10, and the limonic acid (LA) + OH reaction had rate constants of  $(1.3 \pm 0.3) \times 10^{10} \text{ M}^{-1} \text{ s}^{-1}$  at pH 2 and  $(5.7 \pm 0.6) \times 10^9 \text{ M}^{-1} \text{ s}^{-1}$  at pH 10.<sup>31,41</sup> Therefore, it is important to control the pH to determine the rate constant of the reaction of VA with OH radicals. Kinetic plots were obtained under acidic (pH 2) and basic (pH 10) conditions using the relative rate technique.<sup>29</sup> Linear regression analysis was used to calculate the  $k/k_{\text{ref}}$  values, and the kinetic data acquired over three runs in this work are given Table S2 in the Supporting Information.

The fitted slopes in Figure 1 were used to calculate the rate constants. The rate constants of the VA + OH reaction are determined to be  $(9.8 \pm 1.5) \times 10^9$  and  $(3.8 \pm 0.7) \times 10^9 \text{ M}^{-1} \text{ s}^{-1}$  in solution at pH 2 and 10, respectively. A previous study reported the oxidation of *cis*-pinonic acid by OH radicals, and a small rate constant was obtained under acidic conditions. The higher reactivity of VA is most likely due to oxidation of the phenolic OH group, which is missing from the structure of *cis*-pinonic acid. However, the rate constant for limonic acid, an unsaturated carboxylic acid, is larger than that for VA, because the reactivity of the double bond in limonic acid is higher than that of the OH group of VA.<sup>31</sup>

The data in Table S2 show that the reactivity of VA under acidic conditions is higher than that under basic conditions. However, current research results for methoxyphenolic acids oxidation by OH radicals in the aqueous phase are quite limited. The rate constants obtained from previous laboratory studies for the reaction of OH radicals with carboxylic acid compounds and aromatic compounds are summarized in Table 1. It is obvious that the increased rate constants of phenol/methoxyphenol + OH reactions were obtained with increased pH values (Table 1). For example, the rate constants for the catechol + OH reaction were  $(2.5 \pm 0.3) \times 10^9 \text{ M}^{-1} \text{ s}^{-1}$  at pH 2 and  $1.1 \times 10^{10} \text{ M}^{-1} \text{ s}^{-1}$  at pH 9.<sup>42</sup> The literature suggests that it might be caused by the acidity at pH 2 preventing OH radicals from attacking phenol.<sup>43</sup> However, the data listed in Table 1 indicate that the reactivity of the protonated (pH 2) form of the carbonyl acids toward OH radicals is generally higher than the reactivity of the corresponding carboxylate

anions (pH 8 or 10). On the basis of the structure-activity relationship prediction, dissociation of the carboxylic group should increase the overall *cis*-pinonic acid reactivity toward OH radicals, whereas deprotonation of the  $-\text{CH}_3$  group most likely counteracts the increased reactivity of *cis*-pinonic acid, which leads to the rate constant at pH 2 being higher than that at pH 10.<sup>44</sup> Meanwhile, the aqueous structure-activity relationship prediction is unable to account for the neighboring effects of the dissociated aliphatic hydrogen atoms. Therefore, no pH dependence of the rate constant was observed for the reactions of carboxylic acids in previous studies.<sup>26,30</sup> Although VA is an aromatic compound, it is also a carboxylic acid compound and will show different forms under acidic and basic conditions. It is difficult to estimate the pH dependence on the rate constant of the VA + OH reaction. While we did not experimentally explore the mechanism for the pH effect, the difference of rate constants between acidic and basic conditions is likely caused by the differences in favorable reaction pathways. Further studies are still needed to obtain a more general conclusions about the reactivity of carboxylic acid compounds toward OH radicals at different pH values.

It can be noted that creosol, syringol, and 3-methoxycatechol undergo faster reactions with OH radicals than guaiacol and 3-methoxyphenol (Table 1).<sup>32</sup> Compared to monosubstituted phenols (guaiacol and 3-methoxyphenol), creosol ( $-\text{CH}_3$ ), syringol ( $-\text{OCH}_3$ ), and 3-methoxycatechol ( $-\text{OH}$ ) have an additional electron-donating group. The electron-donating group not only makes the benzene ring more likely to participate in electrophilic OH-addition reactions but also provides more hydrogens for potential H-abstraction reactions.<sup>32</sup> The rate constant of the 3-methoxycatechol reaction with OH radicals is higher than those of creosol and syringol, which can be attributed to the stronger electron-donating ability of the additional  $-\text{OH}$  group than  $-\text{CH}_3$  and  $-\text{OCH}_3$ . Similarly, the rate constant of resorcinol reaction with OH radicals is higher than that of 3-methoxyphenol.<sup>32</sup> In summary, 3-methoxyphenol with an additional electron-donating group is the most susceptible to react with OH radicals.

**UV-vis Spectra.** BrC species in particles can absorb a significant amount of sunlight in the atmosphere, and biomass burning is an important source of BrC.<sup>43,45</sup> Interestingly, the reaction solution of VA + OH changes from transparent to

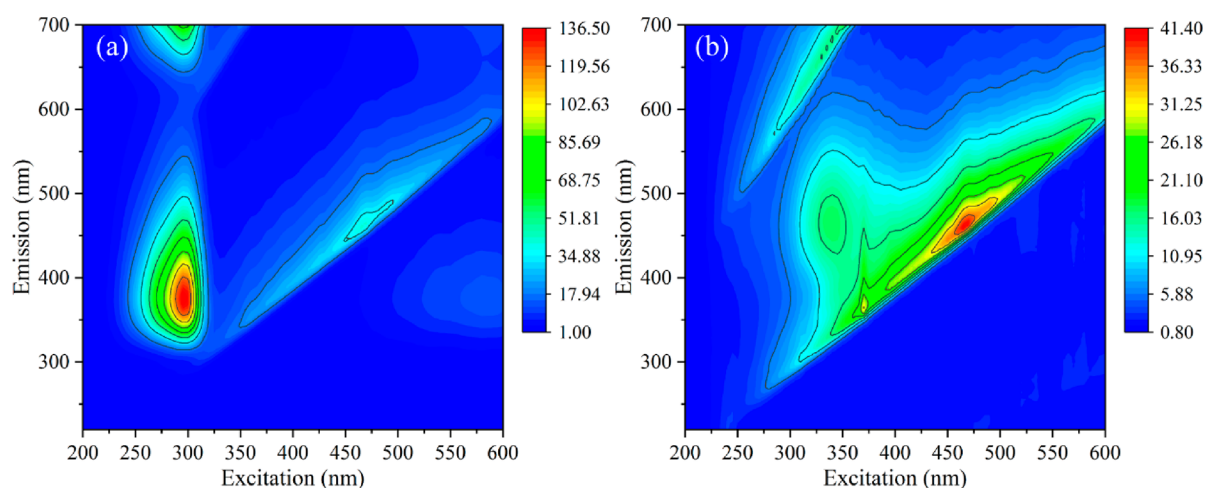


**Figure 3.** Excitation–emission matrix (EEM) spectra of vanillic acid oxidized by OH radicals in the aqueous phase at pH 2 before (a) and after 210 min (b) irradiation.

yellow after illumination (Figure S6); thus, UV–vis spectral analysis was used to determine how the illumination of aqueous phenolic acid affects its light absorption. Time-dependent absorption spectra of the reaction solutions of VA and OH radicals at pH 2 and 10 are shown in Figures 2 and S7, respectively. VA absorbs at 260 and 292 nm (pH 2), corresponding to the  $\pi \rightarrow \pi^*$  ( $>180$  nm) and  $n \rightarrow \pi^*$  (270–350 nm) electronic transitions, respectively.<sup>46,47</sup> Under basic conditions, the  $\pi \rightarrow \pi^*$  and  $n \rightarrow \pi^*$  electronic transitions deviate slightly and are observed at 253 and 288 nm, respectively (Figure S7a).

As shown in Figure 2a, VA undergoes fast photo-transformation under illumination. The absorbances of the initial peaks at 260 and 292 nm undergo a rapid loss. At the same time, the overall shape of the absorption spectrum changes with an increase in the absorption in the long UV (370–400 nm) and visible regions, in which VA does not absorb light. The appearance of new absorption bands in this range agrees well with the experimental findings of a previous study of the Fenton-like oxidation of VA in an atmospheric aqueous phase,<sup>47</sup> in which an increase in the absorption at 400 nm was reported.<sup>47</sup> To observe the absorption at  $\lambda > 320$  nm more clearly, oxidation of VA by OH radicals was performed at a larger VA concentration (5 mM), as shown in the inset of Figure 2a. The absorption in the visible region is significant and extends up to 600 nm. The increase in the absorption spectra in this region results from formation of oligomeric products, which have large, conjugated  $\pi$ -electron structures.<sup>24</sup> A very minor consumption of VA in the absence of OH precursors under 2 h irradiation was observed in this study. Therefore, the appearance of additional absorption bands at longer wavelengths mainly results from the aqueous-phase oxidation of VA by OH radicals. The highly absorbing phenolic acid transforms into other forms of BrC that absorb less efficiently. However, it is worth noting that the mass absorption coefficients of phenolic carbonyl SOA are much higher than those of gas-phase SOA precursors.<sup>48,49</sup>

The absorption bands at 260, 292, and 320 nm measured at pH 2 are plotted as a function of irradiation time in Figure 2b. The absorption at the longer wavelength (320 nm) first increases and then decreases. Finally, almost no UV absorption occurs after 300 min of irradiation. A similar phenomenon was observed for the Fenton-like reaction of VA in an atmospheric

aqueous phase.<sup>47</sup> The increase in the absorption indicates formation of new chromophores. The subsequent decrease in the absorption might indicate the degradation of the produced compounds.<sup>47</sup> A photobleaching process has been observed during secondary BrC aging in many studies, and the atmospheric lifetimes ranged from minutes to several hours.<sup>47,50–52</sup> The UV–vis spectra of fulvic acid solutions decayed at longer  $\lambda$  values with increasing irradiation time due to the photodegradation of dissolved organic matter.<sup>52</sup> Furthermore, some previous studies of the effects of aging on primary BrC demonstrated that BrC formed from biomass burning can undergo both photoenhancement and photobleaching.<sup>51,53,54</sup> The dynamic nature of biomass burning BrC during aging was illustrated in these studies, but the mechanisms remain unclear, including the manner in which biomass burning BrC responds to photolytic aging and the photolytic aging effects for different classes of compounds.

Wu et al. isolated and analyzed HULIS from total suspended particulate samples from Nam Co, and they suggested that HULIS from biomass burning emissions absorbs light in the UV to visible wavelength range.<sup>55</sup> HULIS was also extracted from smoke PM<sub>2.5</sub> emitted during biomass material combustion and from atmospheric aerosols, and its UV–vis absorption decreased as the wavelength increased.<sup>19,44,56</sup> It was verified to be primary humic substances with absorption in the long wavelength.<sup>57</sup> Atmospheric HULIS was recognized as an important component of BrC. It has been found that irradiation of aqueous mixtures containing H<sub>2</sub>O<sub>2</sub> and phenolic compounds results in formation of visible light-absorbing solutions.<sup>24</sup> The colored solutions formed are similar to HULIS in atmospheric particulate matter. On the other hand, the rate of formation of colored products is faster for *o*-methoxy-substituted phenols, such as VA, due to the electron-donating nature of the methoxy group.<sup>24</sup> Therefore, the absorption in the long UV to visible region observed in the VA + OH reaction is likely caused by formation of HULIS, and the secondary HULIS has light absorption properties similar to HULIS in smoke PM<sub>2.5</sub> and atmospheric aerosols.

**Fluorescence Spectra.** Fluorescence spectroscopy has been widely used to characterize HULIS in ambient aerosol particles because of its ability to distinguish and classify humic substances of various origins and natures.<sup>19,58</sup> The fluorescence spectra of VA oxidized by OH radicals at pH 2 before and after

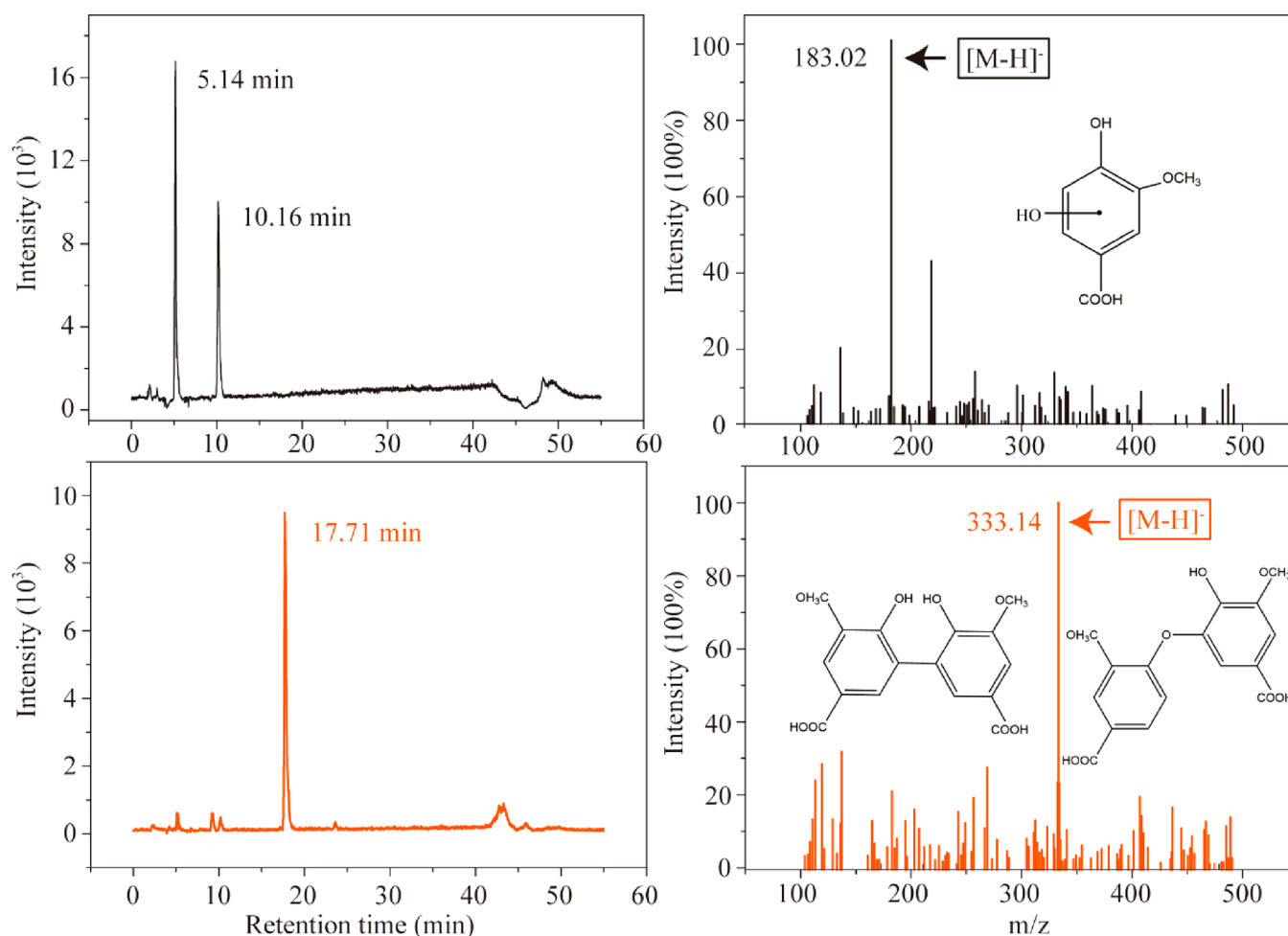


**Figure 4.** Extracted ion current (EIC) chromatograms and mass spectra of two major products identified by HPLC-MS.

illumination are presented in Figure 3. In general, the sample fluoresces with emission maxima in the range of 325–425 nm when excited at 280 nm.<sup>24</sup> As expected, the parent compound exhibits fluorescence (Figure 3a), which is consistent with the fluorescence feature of primary HULIS in smoke PM<sub>2.5</sub> ( $\lambda_{\text{ex}}/\lambda_{\text{em}} \approx 280/350$  nm).<sup>19</sup> The variations in the emission spectra were noted to be a result of the reaction. In this study, a new fluorescence peak can be observed at the excitation (Ex)/emission (Em) wavelengths Ex/Em = 350/450 nm, which corresponds to the spectral regions of the C peak (visible excitation) of humic substances. Additionally, the fluorescence maximum moves from Ex/Em = 250–300/300–500 nm to Ex/Em = 400–500/400–500 nm (Figure 3). The EEM signal exhibits a bathochromic shift after illumination, which is often associated with increasing conjugation.<sup>24</sup> The primary HULIS in smoke PM<sub>2.5</sub> did not exhibit EEM fluorescence in this region, which suggests that the fluorescence spectra presented in Figure 3b are likely due to secondary HULIS from the reaction.

Similar to the UV–vis spectral analysis, no new fluorescence peaks were observed for the products of the photolysis of vanillic acid in a previous study; only acetosyringone and vanillin photolysis led to the appearance of fluorescence signals of humic-like species.<sup>25</sup> In addition, photochemical oxidation and direct photolysis of vanillin resulted in a yellowish solution (high-molecular-weight products), which demonstrates that the reaction of methoxyphenol in the aqueous phase can lead

to a substantial amount of SOA formation. Those results confirm that formation of a yellowish solution after irradiation of vanillic acid in this study is due to photochemical oxidation by OH radicals, rather than photolysis.

The fluorescence spectrum of atmospheric aerosol HULIS is broad (300–500 nm), often with a peak emission near 400 nm.<sup>37</sup> A previous study demonstrated that acetosyringone and vanillin can undergo photolysis and exhibit similar phenomena (absorbance increase at  $\lambda > 350$  nm, appearance of humic-like fluorescence spectra).<sup>25</sup> Direct photolysis of tyrosine and 4-phenoxyphenol generated new fluorescence signals at Ex/Em = 200–250/400–450 nm and 300/400–450 nm, which were attributed to humic substances.<sup>38</sup> For some phenolic compounds that do not undergo photolysis, the fluorescence spectra of the reaction products of their oxidation by OH radicals have similar properties to those of aerosol HULIS.<sup>24</sup> In those previous studies, HULIS formation was derived from formation of dimers of the reactants. Moreover, theoretical calculations illustrated that if oligomers are formed, it is highly possible that they emit fluorescence at approximately 400 nm.<sup>39</sup> Although it is difficult to compare the fluorescence spectra of secondary reaction products with those of aerosol HULIS, some similarities are detected. The oxidation products of VA + OH likely contain HULIS based on UV–vis and fluorescence analyses. In addition, it should be noted that the emission spectra can be influenced by the solution pH, which can affect the ionization degree, inter- and intramolecular

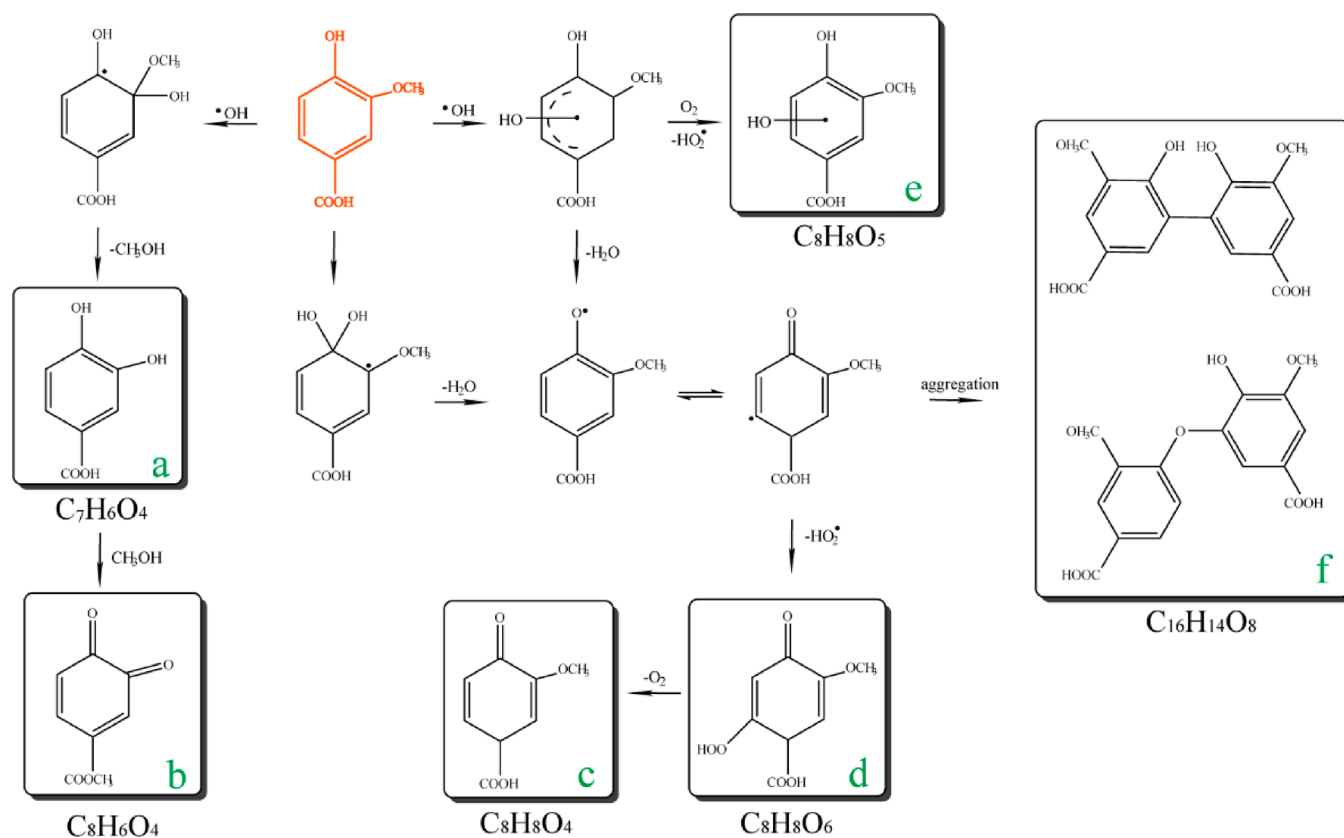


**Figure 5.** Proposed reaction mechanism and product structures of vanillic acid oxidized by OH radicals in the aqueous phase.

bondings, and configurational and structural rearrangement of the functional groups. These factors are responsible for the fluorescence in the humic macromolecules.<sup>59</sup> Therefore, the fluorescence spectra exhibit some differences at pH 10 (Figure S8).

**Mechanism of Vanillic Acid Oxidation by OH Radicals.** ESI-MS measurements were performed in both positive- and negative-ion modes. The products of the VA + OH reaction were identified from the negative-ion mode results. ESI is a “soft” ionization technique in which samples often form protonated or deprotonated ions. The extracted ion chromatograms and mass spectra of some of the products identified by HPLC-ESI-MS are illustrated in Figure 4. Additional mass spectra are shown in Figure S9. The same products were obtained at pH 2 and 10, which is consistent with previous studies.<sup>31,41</sup> Considering that pH 2 is close to real atmospheric conditions, the product formation mechanism in Figure 5 is based on the protonated form of VA.

A number of monomeric products (Figure 5), including a–e with molecular formulas of  $\text{C}_7\text{H}_6\text{O}_4$ ,  $\text{C}_8\text{H}_6\text{O}_4$ ,  $\text{C}_8\text{H}_8\text{O}_4$ ,  $\text{C}_8\text{H}_8\text{O}_6$ , and  $\text{C}_8\text{H}_8\text{O}_5$ , are observed after 60 min of reaction. Of these, product a ( $\text{C}_7\text{H}_6\text{O}_4$ , 3,4-dihydroxybenzoic acid) was previously identified in the Fenton-like oxidation of VA in the aqueous phase<sup>47</sup> and in the ozonolysis of coniferyl alcohol under simulated solar light.<sup>60</sup> In addition, two chromatographic peaks detected at  $m/z$  183.02 ion with retention times of 5.14 and 10.16 min (Figure 4) are most likely due to formation of two isomers of compound e. The  $m/z$  183.02 ion is most likely produced by an addition mechanism (Figure 5). The isomers might be different hydroxyl-substituted VA derivatives with a hydroxyl group, in addition to the original one, at one of the two available positions on the aromatic ring.

Similar isomers of hydroxyl-substituted derivatives were also identified in the oxidation of limonic acid by OH radicals<sup>31</sup> and the photolysis of vanillin<sup>12</sup> in the aqueous phase. The addition mechanism is expected to be the main mechanism instead H-atom abstraction;<sup>31</sup> thus, the addition product transforms into an alkoxy radical by eliminating one water molecule, and no products are formed by the abstraction mechanism in this study.

Several products with longer retention times (17.71 min) are observed, as shown in Figure 4. The oligomeric products with the molecular formula  $\text{C}_{16}\text{H}_{14}\text{O}_8$  at  $m/z$  333.14 (Figure 5) are believed to be dimers formed via radical–radical polymerization. The mass increment can be explained by the condensation of two phenoxyl radicals.<sup>16,61</sup> After the phenolic proton is abstracted by an OH radical, delocalization would be predicted based on resonance theory, and then carbon radicals would form at other sites on the aromatic ring. In this way, two radicals could possibly couple through the C–C and C–O linkages to yield higher molecular weight products.<sup>62</sup> Using Fourier transform ion cyclotron resonance mass spectrometry (FT-ICR-MS), similar oligomers were detected during the photolysis of vanillin, and humic-like fluorescence was also observed.<sup>25</sup> However, no oligomers were detected during the photolysis of VA,<sup>25</sup> confirming that the oligomers are formed by the reaction of VA with OH radicals during the photochemical reaction rather than by direct photolysis. Additionally, oligomeric products with large, conjugated  $\pi$ -electron systems and light absorption at long wavelengths, which is consistent with humic-like substances, were identified after the oxidation of phenolic compounds.<sup>24</sup> VA yields oligomeric species that absorb in the long UV and visible regions and exhibit unusual fluorescence behavior (EEM  $\lambda_{\text{ex}}/$

$\lambda_{em} \approx 450/450$  nm) upon oxidation by OH radicals, which results from the possible formation of HULIS candidates. The structure of the oligomeric species is formed by two phenoxy radicals and is shown in Figure 5 ( $m/z$  333.14 ion).

Additional reaction pathways involving demethylation ( $-OCH_3 \rightarrow -OH$ ) and hydroxyl oxidation ( $-OH \rightarrow =O$ ) should also be considered for obtaining highly oxidized products with an increase (or at least similar) in the double-bond equivalence (DBE) relative to VA. By adding OH to the carbon atom with the  $-OCH_3$  group and subsequently eliminating  $CH_3OH$ , the  $m/z$  153.07 ion is formed (demethylation). The  $m/z$  153.07 ion can be converted to a quinone compound, which can also undergo esterification pathways in the presence of  $CH_3OH$ . These pathways are often observed in photochemical processes.<sup>4,30,63</sup> Clearly, the VA + OH reaction might result in formation of other products, but they are most likely not detected here due to the limitations of the LC-MS instrument and its separation column.

**Atmospheric Implication.** The kinetics, optical properties, and possible mechanism of the photochemical oxidation of vanillic acid by OH radicals in the aqueous phase were investigated by HPLC–UV/MS. Two interesting phenomena are observed. First, the rate constants of the VA + OH reaction are  $(9.8 \pm 1.5) \times 10^9$  and  $(3.8 \pm 0.7) \times 10^9$   $M^{-1} s^{-1}$  at pH 2 and 10, respectively. The atmospheric aqueous-phase lifetimes ( $\tau$ ) of the VA + OH reaction can be calculated using the following equation<sup>64</sup>

$$\tau = \frac{1}{k_{VA} \times [OH]} \quad (4)$$

The mean OH concentration in remote cloud droplets is  $2.2 \times 10^{-14}$  M.<sup>65</sup> The lifetimes are calculated to be approximately 1.29 and 3.37 h at pH 2 and 10, respectively, which indicates that vanillic acid is consumed more quickly at pH 2 when reacting with OH radicals. Despite the fact that the rate constant under acidic conditions is obviously larger than that under basic conditions, it is difficult to estimate the pH dependence of the rate constant. Further experiments are needed to investigate the relation between the rate constant and the aqueous pH for different classes of compounds.

Second, a yellowish solution that absorbs in the UV–vis region and has an unusual fluorescence spectrum is observed after illumination, which might be due to formation of high-molecular-weight products by radical–radical polymerization. The second phenomenon suggests that OH oxidation of methoxyphenolic acids could contribute to light-absorbing HULIS. These high-molecular-weight compounds tend to preferentially form at high reactant concentrations.<sup>66,67</sup> There are two limitations in the present study: (1) the VA concentration used in this study is higher than its atmospheric concentration; (2) the UV light (254 nm) used here is different from actinic radiation in the ambient atmosphere (>290 nm). However, the ice core records of VA from Aurora Peak in Alaska since the 1660s reveal that the enhanced emissions of the biomass burning products of conifer trees and lignin in boreal forests can increase the concentration of VA.<sup>28</sup> Therefore, OH oxidation of biomass burning emissions is likely a potential source of HULIS formation in the woody aerosol phase. Given that phenolic aqSOA is both water soluble and light absorbing, these aqueous reactions might significantly modify the chemical compositions and optical properties of atmospheric particles in regions influenced by biomass burning

emissions and further impact the climate and human health. In the future, more work is needed to better integrate different real atmospheric conditions (intermediate pH values) to validate atmospheric chemistry processes.

## ■ ASSOCIATED CONTENT

### Supporting Information

The Supporting Information is available free of charge at <https://pubs.acs.org/doi/10.1021/acsearthspacechem.0c00070>.

Gradient elution program; relative kinetic data for aqueous reaction of vanillic acid (VA) with OH radicals under acidic and basic conditions; emission spectrum of the used UV lamp; loss of vanillic acid as the reaction progressed; UV–vis absorption spectra of vanillic acid; control experiments; calibration curve of vanillic acid; solution color; UV–vis absorption spectra of vanillic acid oxidized by OH radicals under pH 10; EEM spectra of vanillic acid oxidized by OH radicals under pH 10; mass spectra of some products (PDF)

## ■ AUTHOR INFORMATION

### Corresponding Author

Lin Du – Environment Research Institute, Shandong University, Qingdao 266237, China; [orcid.org/0000-0001-8208-0558](https://orcid.org/0000-0001-8208-0558); Email: [lindu@sdu.edu.cn](mailto:lindu@sdu.edu.cn)

### Authors

Shanshan Tang – Environment Research Institute, Shandong University, Qingdao 266237, China; [orcid.org/0000-0002-4121-8239](https://orcid.org/0000-0002-4121-8239)

Fenghua Li – Environment Research Institute, Shandong University, Qingdao 266237, China

Narcisse T. Tsona – Environment Research Institute, Shandong University, Qingdao 266237, China; [orcid.org/0000-0002-6023-1850](https://orcid.org/0000-0002-6023-1850)

Chunying Lu – Environment Research Institute, Shandong University, Qingdao 266237, China

Xinfeng Wang – Environment Research Institute, Shandong University, Qingdao 266237, China; [orcid.org/0000-0003-0911-7312](https://orcid.org/0000-0003-0911-7312)

Complete contact information is available at:

<https://pubs.acs.org/doi/10.1021/acsearthspacechem.0c00070>

### Notes

The authors declare no competing financial interest.

## ■ ACKNOWLEDGMENTS

This work was supported by National Natural Science Foundation of China (91644214), Shandong Natural Science Fund for Distinguished Young Scholars (JQ201705), Youth Innovation Program of Universities in Shandong Province (2019KJD007), and Fundamental Research Fund of Shandong University (2020QNQT012).

## ■ REFERENCES

- (1) Kroll, J. H.; Seinfeld, J. H. Chemistry of Secondary Organic Aerosol: Formation and Evolution of Low-Volatility Organics in the Atmosphere. *Atmos. Environ.* **2008**, *42* (16), 3593–3624.
- (2) Hallquist, M.; Wenger, J. C.; Baltensperger, U.; Rudich, Y.; Simpson, D.; Claeys, M.; Dommen, J.; Donahue, N. M.; George, C.; Goldstein, A. H.; Hamilton, J. F.; Herrmann, H.; Hoffmann, T.; Iinuma, Y.; Jang, M.; Jenkin, M. E.; Jimenez, J. L.; Kiendler-Scharr, A.;

- Maenhaut, W.; McFiggans, G.; Mentel, T. F.; Monod, A.; Prevot, A. S. H.; Seinfeld, J. H.; Surratt, J. D.; Szmigielski, R.; Wildt, J. The Formation, Properties and Impact of Secondary Organic Aerosol: Current and Emerging Issues. *Atmos. Chem. Phys.* **2009**, *9* (14), 5155–5236.
- (3) Blando, J. D.; Turpin, B. J. Secondary Organic Aerosol Formation in Cloud and Fog Droplets: A Literature Evaluation of Plausibility. *Atmos. Environ.* **2000**, *34* (10), 1623–1632.
- (4) Herrmann, H.; Schaefer, T.; Tilgner, A.; Styler, S. A.; Weller, C.; Teich, M.; Otto, T. Tropospheric Aqueous-Phase Chemistry: Kinetics, Mechanisms, and Its Coupling to a Changing Gas Phase. *Chem. Rev.* **2015**, *115* (10), 4259–4334.
- (5) Ervens, B. Modeling the Processing of Aerosol and Trace Gases in Clouds and Fogs. *Chem. Rev.* **2015**, *115* (10), 4157–4198.
- (6) McNeill, V. F. Aqueous Organic Chemistry in the Atmosphere: Sources and Chemical Processing of Organic Aerosols. *Environ. Sci. Technol.* **2015**, *49* (3), 1237–1244.
- (7) Gilardoni, S.; Massoli, P.; Paglione, M.; Giulianelli, L.; Carbone, C.; Rinaldi, M.; Decesari, S.; Sandrini, S.; Costabile, F.; Gobbi, G. P.; Pietrogrande, M. C.; Visentin, M.; Scotto, F.; Fuzzi, S.; Facchini, M. C. Direct Observation of Aqueous Secondary Organic Aerosol from Biomass-Burning Emissions. *Proc. Natl. Acad. Sci. U. S. A.* **2016**, *113* (36), 10013–8.
- (8) De Gouw, J.; Jimenez, J. L. Organic Aerosols in the Earth's Atmosphere. *Environ. Sci. Technol.* **2009**, *43* (20), 7614–7618.
- (9) Simoneit, B. R. T. Biomass Burning — A Review of Organic Tracers for Smoke from Incomplete Combustion. *Appl. Geochem.* **2002**, *17* (3), 129–162.
- (10) Wan, X.; Kawamura, K.; Ram, K.; Kang, S.; Loewen, M.; Gao, S.; Wu, G.; Fu, P.; Zhang, Y.; Bhattarai, H.; Cong, Z. Aromatic Acids as Biomass-Burning Tracers in Atmospheric Aerosols and Ice Cores: A Review. *Environ. Pollut.* **2019**, *247*, 216–228.
- (11) Hawthorne, S. B.; Krieger, M. S.; Miller, D. J.; Mathiason, M. B. Collection and Quantitation of Methoxylated Phenol Tracers for Atmospheric Pollution from Residential Wood Stoves. *Environ. Sci. Technol.* **1989**, *23* (4), 470–475.
- (12) Li, Y. J.; Huang, D. D.; Cheung, H. Y.; Lee, A. K. Y.; Chan, C. K. Aqueous-Phase Photochemical Oxidation and Direct Photolysis of Vanillin — A Model Compound of Methoxy Phenols from Biomass Burning. *Atmos. Chem. Phys.* **2014**, *14* (6), 2871–2885.
- (13) Yu, L.; Smith, J.; Laskin, A.; George, K. M.; Anastasio, C.; Laskin, J.; Dillner, A. M.; Zhang, Q. Molecular Transformations of Phenolic SOA during Photochemical Aging in the Aqueous Phase: Competition among Oligomerization, Functionalization, and Fragmentation. *Atmos. Chem. Phys.* **2016**, *16* (7), 4511–4527.
- (14) Tomaz, S.; Cui, T.; Chen, Y.; Sexton, K. G.; Roberts, J. M.; Warneke, C.; Yokelson, R. J.; Surratt, J. D.; Turpin, B. J. Photochemical Cloud Processing of Primary Wildfire Emissions as a Potential Source of Secondary Organic Aerosol. *Environ. Sci. Technol.* **2018**, *52* (19), 11027–11037.
- (15) Yu, L.; Smith, J.; Laskin, A.; Anastasio, C.; Laskin, J.; Zhang, Q. Chemical Characterization of SOA Formed from Aqueous-Phase Reactions of Phenols with the Triplet Excited State of Carbonyl and Hydroxyl Radical. *Atmos. Chem. Phys.* **2014**, *14* (24), 13801–13816.
- (16) Sun, Y. L.; Zhang, Q.; Anastasio, C.; Sun, J. Insights into Secondary Organic Aerosol formed via Aqueous-Phase Reactions of Phenolic Compounds Based on High Resolution Mass Spectrometry. *Atmos. Chem. Phys.* **2010**, *10* (10), 4809–4822.
- (17) George, K. M.; Ruthenburg, T. C.; Smith, J.; Yu, L.; Zhang, Q.; Anastasio, C.; Dillner, A. M. FT-IR Quantification of the Carbonyl Functional Group in Aqueous-Phase Secondary Organic Aerosol from Phenols. *Atmos. Environ.* **2015**, *100*, 230–237.
- (18) Budisulistiorini, S. H.; Riva, M.; Williams, M.; Chen, J.; Itoh, M.; Surratt, J. D.; Kuwata, M. Light-Absorbing Brown Carbon Aerosol Constituents from Combustion of Indonesian Peat and Biomass. *Environ. Sci. Technol.* **2017**, *51* (8), 4415–4423.
- (19) Fan, X.; Wei, S.; Zhu, M.; Song, J.; Peng, P. Comprehensive Characterization of Humic-Like Substances in Smoke PM<sub>2.5</sub> Emitted from the Combustion of Biomass Materials and Fossil Fuels. *Atmos. Chem. Phys.* **2016**, *16* (20), 13321–13340.
- (20) Li, C.; He, Q.; Schade, J.; Passig, J.; Zimmermann, R.; Meidan, D.; Laskin, A.; Rudich, Y. Dynamic Changes in Optical and Chemical Properties of Tar Ball Aerosols by Atmospheric Photochemical Aging. *Atmos. Chem. Phys.* **2019**, *19* (1), 139–163.
- (21) Schnitzler, E. G.; Abbatt, J. P. D. Heterogeneous OH Oxidation of Secondary Brown Carbon Aerosol. *Atmos. Chem. Phys.* **2018**, *18* (19), 14539–14553.
- (22) Laskin, A.; Laskin, J.; Nizkorodov, S. A. Chemistry of Atmospheric Brown Carbon. *Chem. Rev.* **2015**, *115* (10), 4335–4382.
- (23) Gelencsér, A.; Hoffer, A.; Kiss, G.; Tombácz, E.; Kurdi, R.; Bencze, L. In-situ Formation of Light-Absorbing Organic Matter in Cloud Water. *J. Atmos. Chem.* **2003**, *45* (1), 25–33.
- (24) Chang, J. L.; Thompson, J. E. Characterization of Colored Products Formed during Irradiation of Aqueous Solutions Containing H<sub>2</sub>O<sub>2</sub> and Phenolic Compounds. *Atmos. Environ.* **2010**, *44* (4), 541–551.
- (25) Vione, D.; Albinet, A.; Barsotti, F.; Mekic, M.; Jiang, B.; Minero, C.; Brigante, M.; Gligorovski, S. Formation of Substances with Humic-Like Fluorescence Properties, upon Photoinduced Oligomerization of Typical Phenolic Compounds Emitted by Biomass Burning. *Atmos. Environ.* **2019**, *206*, 197–207.
- (26) Simoneit, B. R. T.; Rogge, W. F.; Mazurek, M. A.; Standley, L. J.; Hildemann, L. M.; Cass, G. R. Lignin Pyrolysis Products, Lignans, and Resin Acids as Specific Tracers of Plant Classes in Emissions from Biomass Combustion. *Environ. Sci. Technol.* **1993**, *27* (12), 2533–2541.
- (27) Ren, H.; Kang, M.; Ren, L.; Zhao, Y.; Pan, X.; Yue, S.; Li, L.; Zhao, W.; Wei, L.; Xie, Q.; Li, J.; Wang, Z.; Sun, Y.; Kawamura, K.; Fu, P. The Organic Molecular Composition, Diurnal Variation, and Stable Carbon Isotope Ratios of PM<sub>2.5</sub> in Beijing during the 2014 APEC Summit. *Environ. Pollut.* **2018**, *243*, 919–928.
- (28) Pokhrel, A.; Kawamura, K.; Kunwar, B.; Ono, K.; Tsushima, A.; Seki, O.; Matoba, S.; Shiraiwa, T. Ice Core Records of Levoglucosan and Dehydroabietic and Vanillic Acids from Aurora Peak in Alaska Since the 1660s: A Proxy Signal of Biomass-Burning Activities in the North Pacific Rim. *Atmos. Chem. Phys.* **2020**, *20* (1), 597–612.
- (29) Aljawhary, D.; Zhao, R.; Lee, A. K. Y.; Wang, C.; Abbatt, J. P. D. Kinetics, Mechanism, and Secondary Organic Aerosol Yield of Aqueous Phase Photo-oxidation of  $\alpha$ -Pinene Oxidation Products. *J. Phys. Chem. A* **2016**, *120* (9), 1395–1407.
- (30) Witkowski, B.; Al-sharafi, M.; Gierczak, T. Kinetics and products of the aqueous-phase oxidation of  $\beta$ -caryophyllonic acid by hydroxyl radicals. *Atmos. Environ.* **2019**, *213*, 231–238.
- (31) Witkowski, B.; Jurdana, S.; Gierczak, T. Limononic Acid Oxidation by Hydroxyl Radicals and Ozone in the Aqueous Phase. *Environ. Sci. Technol.* **2018**, *52* (6), 3402–3411.
- (32) He, L.; Schaefer, T.; Otto, T.; Kroflič, A.; Herrmann, H. Kinetic and Theoretical Study of the Atmospheric Aqueous-Phase Reactions of OH Radicals with Methoxyphenolic Compounds. *J. Phys. Chem. A* **2019**, *123* (36), 7828–7838.
- (33) Ervens, B.; Gligorovski, S.; Herrmann, H. Temperature-Dependent Rate Constants for Hydroxyl Radical Reactions with Organic Compounds in Aqueous Solutions. *Phys. Chem. Chem. Phys.* **2003**, *5* (9), 1811–1824.
- (34) Erdemgil, F. Z.; Şanlı, S.; Şanlı, N.; Özkan, G.; Barbosa, J.; Güteras, J.; Beltrán, J. L. Determination of pKa Values of Some Hydroxylated Benzoic Acids in Methanol–Water Binary Mixtures by LC Methodology and Potentiometry. *Talanta* **2007**, *72* (2), 489–496.
- (35) Ozkorucuklu, S. P.; Beltran, J. L.; Fonrodona, G.; Barron, D.; Alsancak, G.; Barbosa, J. Determination of Dissociation Constants of Some Hydroxylated Benzoic and Cinnamic Acids in Water from Mobility and Spectroscopic Data Obtained by CE-DAD. *J. Chem. Eng. Data* **2009**, *54* (3), 807–811.
- (36) Buxton, G. V.; Greenstock, C. L.; Helman, W. P.; Ross, A. B. Critical Review of Rate Constants for Reactions of Hydrated Electrons, Hydrogen Atoms and Hydroxyl Radicals ( $\cdot\text{OH}/\cdot\text{O}^-$ ) in Aqueous Solution. *J. Phys. Chem. Ref. Data* **1988**, *17* (2), 513–886.

- (37) Krivácsy, Z.; Kiss, G.; Ceburnis, D.; Jennings, G.; Maenhaut, W.; Salma, I.; Shooter, D. Study of Water-Soluble Atmospheric Humic Matter in Urban and Marine Environments. *Atmos. Res.* **2008**, *87* (1), 1–12.
- (38) Bianco, A.; Minella, M.; De Laurentiis, E.; Maurino, V.; Minero, C.; Vione, D. Photochemical Generation of Photoactive Compounds with Fulvic-Like and Humic-Like Fluorescence in Aqueous Solution. *Chemosphere* **2014**, *111*, 529–536.
- (39) Barsotti, F.; Ghigo, G.; Vione, D. Computational Assessment of the Fluorescence Emission of Phenol Oligomers: A Possible Insight into the Fluorescence Properties of Humic-Like Substances (HULIS). *J. Photochem. Photobiol., A* **2016**, *315*, 87–93.
- (40) Kramp, F.; Paulson, S. E. On the Uncertainties in the Rate Coefficients for OH Reactions with Hydrocarbons, and the Rate Coefficients of the 1,3,5-Trimethylbenzene and m-Xylene Reactions with OH Radicals in the Gas Phase. *J. Phys. Chem. A* **1998**, *102* (16), 2685–2690.
- (41) Witkowski, B.; Gierczak, T. cis-Pinonic Acid Oxidation by Hydroxyl Radicals in the Aqueous Phase under Acidic and Basic Conditions: Kinetics and Mechanism. *Environ. Sci. Technol.* **2017**, *51* (17), 9765–9773.
- (42) Smith, J. D.; Kinney, H.; Anastasio, C. Aqueous Benzene-diols React with An Organic Triplet Excited State and Hydroxyl Radical to Form Secondary Organic Aerosol. *Phys. Chem. Chem. Phys.* **2015**, *17* (15), 10227–10237.
- (43) Smith, J. D.; Kinney, H.; Anastasio, C. Phenolic carbonyls undergo rapid aqueous photodegradation to form low-volatility, light-absorbing products. *Atmos. Environ.* **2016**, *126*, 36–44.
- (44) Fan, X.; Song, J.; Peng, P. Comparison of Isolation and Quantification Methods to Measure Humic-Like Substances (HULIS) in Atmospheric Particles. *Atmos. Environ.* **2012**, *60*, 366–374.
- (45) Chen, Y.; Bond, T. C. Light Absorption by Organic Carbon from Wood Combustion. *Atmos. Chem. Phys.* **2010**, *10* (4), 1773–1787.
- (46) Yi, Y.; Zhou, X.; Xue, L.; Wang, W. Air Pollution: Formation of Brown, Light-Absorbing, Secondary Organic Aerosols by Reaction of Hydroxyacetone and Methylamine. *Environ. Chem. Lett.* **2018**, *16* (3), 1083–1088.
- (47) Santos, G. T. A. D.; Santos, P. S. M.; Duarte, A. C. Vanillic and Syringic Acids from Biomass Burning: Behaviour during Fenton-Like Oxidation in Atmospheric Aqueous Phase and in the Absence of Light. *J. Hazard. Mater.* **2016**, *313*, 201–208.
- (48) Nguyen, T. B.; Lee, P. B.; Updyke, K. M.; Bones, D. L.; Laskin, J.; Laskin, A.; Nizkorodov, S. A. Formation of Nitrogen- and Sulfur-Containing Light-Absorbing Compounds Accelerated by Evaporation of Water from Secondary Organic Aerosols. *J. Geophys. Res.-Atmos.* **2012**, *117*, D01207.
- (49) Updyke, K. M.; Nguyen, T. B.; Nizkorodov, S. A. Formation of Brown Carbon via Reactions of Ammonia with Secondary Organic Aerosols from Biogenic and Anthropogenic Precursors. *Atmos. Environ.* **2012**, *63*, 22–31.
- (50) Wong, J. P. S.; Nenes, A.; Weber, R. J. Changes in Light Absorptivity of Molecular Weight Separated Brown Carbon Due to Photolytic Aging. *Environ. Sci. Technol.* **2017**, *51* (15), 8414–8421.
- (51) Zhao, R.; Lee, A. K. Y.; Huang, L.; Li, X.; Yang, F.; Abbott, J. P. D. Photochemical Processing of Aqueous Atmospheric Brown Carbon. *Atmos. Chem. Phys.* **2015**, *15* (11), 6087–6100.
- (52) Otero, M.; Guilherme, I.; Santos, E. B. H. Photobleaching of Lignin Derived Compounds from Pulp Mill Effluents upon Irradiation: The Key Role of Receiving Waters. *Environ. Pollut.* **2013**, *182*, 486–489.
- (53) Saleh, R.; Hennigan, C. J.; McMeeking, G. R.; Chuang, W. K.; Robinson, E. S.; Coe, H.; Donahue, N. M.; Robinson, A. L. Absorptivity of Brown Carbon in Fresh and Photo-chemically Aged Biomass-Burning Emissions. *Atmos. Chem. Phys.* **2013**, *13* (15), 7683–7693.
- (54) Zhong, M.; Jang, M. Dynamic Light Absorption of Biomass-Burning Organic Carbon Photochemically Aged Under Natural Sunlight. *Atmos. Chem. Phys.* **2014**, *14* (3), 1517–1525.
- (55) Wu, G.; Wan, X.; Gao, S.; Fu, P.; Yin, Y.; Li, G.; Zhang, G.; Kang, S.; Ram, K.; Cong, Z. Humic-Like Substances (HULIS) in Aerosols of Central Tibetan Plateau (Nam Co, 4730 m asl): Abundance, Light Absorption Properties, and Sources. *Environ. Sci. Technol.* **2018**, *52* (13), 7203–7211.
- (56) Baduel, C.; Voisin, D.; Jaffrezo, J. L. Seasonal Variations of Concentrations and Optical Properties of Water Soluble HULIS Collected in Urban Environments. *Atmos. Chem. Phys.* **2010**, *10* (9), 4085–4095.
- (57) Domeizel, M.; Khalil, A.; Prudent, P. UV Spectroscopy: A Tool for Monitoring Humification and for Proposing An Index of the Maturity of Compost. *Bioresour. Technol.* **2004**, *94* (2), 177–184.
- (58) Santos, P. S. M.; Santos, E. B. H.; Duarte, A. C. First Spectroscopic Study on the Structural Features of Dissolved Organic Matter Isolated from Rainwater in Different Seasons. *Sci. Total Environ.* **2012**, *426*, 172–179.
- (59) Provenzano, M. R.; Miano, T. M.; Senesi, N. Concentration and pH Effects on the Fluorescence Spectra of Humic Acid-like Soil Fungal Polymers. *Sci. Total Environ.* **1989**, *81–82*, 129–136.
- (60) Net, S.; Alvarez, E. G.; Gligorovski, S.; Wortham, H. Heterogeneous Reactions of Ozone with Methoxyphenols, in Presence and Absence of Light. *Atmos. Environ.* **2011**, *45* (18), 3007–3014.
- (61) Berto, S.; De Laurentiis, E.; Tota, T.; Chiavazza, E.; Daniele, P. G.; Minella, M.; Isaia, M.; Brigante, M.; Vione, D. Properties of the Humic-Like Material Arising from the Photo-Transformation of l-Tyrosine. *Sci. Total Environ.* **2016**, *545–546*, 434–444.
- (62) Lavi, A.; Lin, P.; Bhaduri, B.; Carmieli, R.; Laskin, A.; Rudich, Y. Characterization of Light-Absorbing Oligomers from Reactions of Phenolic Compounds and Fe(III). *ACS Earth Space Chem.* **2017**, *1* (10), 637–646.
- (63) Witkowski, B.; Al-sharafi, M.; Gierczak, T. Ozonolysis of  $\beta$ -Caryophyllonic and Limononic Acids in the Aqueous Phase: Kinetics, Product Yield, and Mechanism. *Environ. Sci. Technol.* **2019**, *53* (15), 8823–8832.
- (64) Otto, T.; Schaefer, T.; Herrmann, H. Aqueous-Phase Oxidation of Terpene-Derived Acids by Atmospherically Relevant Radicals. *J. Phys. Chem. A* **2018**, *122* (47), 9233–9241.
- (65) Herrmann, H.; Hoffmann, D.; Schaefer, T.; Brauer, P.; Tilgner, A. Tropospheric Aqueous-Phase Free-Radical Chemistry: Radical Sources, Spectra, Reaction Kinetics and Prediction Tools. *ChemPhysChem* **2010**, *11* (18), 3796–3822.
- (66) Ervens, B.; Turpin, B. J.; Weber, R. J. Secondary Organic Aerosol Formation in Cloud Droplets and Aqueous Particles (aqSOA): A Review of Laboratory, Field and Model Studies. *Atmos. Chem. Phys.* **2011**, *11* (21), 11069–11102.
- (67) Lim, Y. B.; Tan, Y.; Perri, M. J.; Seitzinger, S. P.; Turpin, B. J. Aqueous Chemistry and Its Role in Secondary Organic Aerosol (SOA) Formation. *Atmos. Chem. Phys.* **2010**, *10* (21), 10521–10539.
- (68) Wu, M.-H.; Liu, N.; Xu, G.; Ma, J.; Tang, L.; Wang, L.; Fu, H.-Y. Kinetics and Mechanisms Studies on Dimethyl Phthalate Degradation in Aqueous Solutions by Pulse Radiolysis and Electron Beam Radiolysis. *Radiat. Phys. Chem.* **2011**, *80* (3), 420–425.
- (69) Wen, G.; Ma, J.; Liu, Z.-Q.; Zhao, L. Ozonation Kinetics for the Degradation of Phthalate Esters in Water and the Reduction of Toxicity in the Process of O<sub>3</sub>/H<sub>2</sub>O<sub>2</sub>. *J. Hazard. Mater.* **2011**, *195*, 371–377.
- (70) Ayatollahi, S.; Kalnina, D.; Song, W.; Turks, M.; Cooper, W. J. Radiation Chemistry of Salicylic and Methyl Substituted Salicylic Acids: Models for the Radiation Chemistry of Pharmaceutical Compounds. *Radiat. Phys. Chem.* **2013**, *92*, 93–98.
- (71) Venu, S.; Naik, D. B.; Sarkar, S. K.; Aravind, U. K.; Nijamudheen, A.; Aravindakumar, C. T. Oxidation Reactions of Thymol: A Pulse Radiolysis and Theoretical Study. *J. Phys. Chem. A* **2013**, *117* (2), 291–299.